J Comput Aided Mol Des (2011) 25:253–262
DOI 10.1007/s10822-011-9417-1

Towards a rational spacer design for bivalent inhibition of estrogen receptor

Alexander Bujotzek · Min Shan · Rainer Haag · Marcus Weber

Received: 19 November 2010 / Accepted: 2 February 2011 / Published online: 18 February 2011

Abstract Estrogen receptors are known drug targets that have been linked to several kinds of cancer. The structure of the estrogen receptor ligand binding domain is available and reveals a homodimeric layout. In order to improve the binding affinity of known estrogen receptor inhibitors, bivalent compounds have been developed that consist of two individual ligands linked by flexible tethers serving as spacers. So far, binding affinities of the bivalent compounds do not surpass their monovalent counterparts. In this article, we focus our attention on the molecular spacers that are used to connect the individual ligands to form bivalent compounds, and describe their thermodynamic contribution during the ligand binding process. We use computational methods to predict structural and entropic parameters of different spacer structures. We find that flexible spacers introduce a number of effects that may interfere with ligand binding and possibly can be connected to the low binding affinities that have been reported in binding assays. Based on these findings, we try to provide guidelines for the design of novel molecular spacers.

Keywords Estrogen receptor · Bivalent ligand · Spacer · Multivalency · Entropy

A. Bujotzek (✉) · M. Weber
Zuse Institute Berlin, Takustraße 7, 14195 Berlin, Germany
e-mail: bujotzek@zib.de

M. Weber
e-mail: weber@zib.de

M. Shan · R. Haag
Institute of Chemistry and Biochemistry, Freie Universität Berlin, Takustraße 3, 14195 Berlin, Germany

Introduction

Estrogen receptor as a drug target

Estrogen receptors (ER) are DNA-binding proteins in the cytoplasm belonging to the superfamily of nuclear receptors (NR). As ligand-dependent transcription factors, they are involved in a variety of processes that regulate gene expression. ER is activated by the estrogen estradiol (E_2), which binds to ER and induces receptor dimerization. The ER dimer is then able to recruit coactivators, bind DNA and regulate gene trancription. E_2 not only regulates female sexual reproduction, but is also involved in regulating tissue growth, development and other physiological functions [1, 24]. It is known that ERs are over-expressed in the majority of breast cancer cases. ERs have also been linked to other kinds of cancer. Ever since, drugs have been developed that bind to ER to prevent the conformational change that is crucial for the recruitment of coactivators [18, 19]. This, in turn, inhibits the transcription process, as ER is unable to establish its DNA binding abilities.

Bivalent inhibition of estrogen receptor

In 1997, Brzozowski et al. first reported the crystal structure of the ER ligand binding domain in complex with endogenous E_2 and the selective estrogen receptor modulator (SERM) raloxifene [5]. This breakthrough provided not only a straightforward method to study the mechanisms of the ER agonistic and antagonistic effect, but also substantial information about the structural parameters of the ER dimer. Moreover, evidence was found that the dimerized form of ER, which has a C2 symmetry, exists even in the absence of the ligand [26]. This finding brought up the possibility for bivalent inhibition of ER. The concept of

multivalency is often used in nature in order to increase weak individual binding affinities by offering multiple interaction sites, e. g. the trimeric hemagglutinin of an influenza virus binding to sialic acids on a bronchial epithelial cell surface [23]. From a thermodynamic point of view, this increase in binding affinity can be attributed to entropic effects. The Gibbs free energy of binding ΔG can be split into an enthalpic and an entropic term, i. e. $\Delta G = \Delta H - T\Delta S$. The enthalpy ΔH largely depends on the nature of the ligand and the binding site of the receptor, which remains invariant with an increase of valency, i. e. $\Delta H_{bi} \approx 2 \times \Delta H_{mono}$. The entropic term, however, which again can be split into translational entropy ΔS_{trans} and rotational entropy ΔS_{rot}, may benefit from bridging the individual ligands with a molecular spacer [23, 25].

Given an idealized model spacer that is completely rigid and yet allows for the ligands to bind with perfect fit, ΔS_{trans} and ΔS_{rot} only have to be accounted for once, as there is no additional entropy cost for the binding of the second ligand. This is exactly half of the cost of the monovalent case, where each individual ligand requires an equivalent of ΔS_{trans} and ΔS_{rot} (see Fig. 1). Consequently, the binding affinity could be maximally increased by entropic optimization. However, the structural parameters for a rigid spacer with perfect fit are very hard to predict and possibly even harder to translate into an actual chemical structure. A small structural mismatch may lead to very weak binding due to unfavorable steric interactions (i. e. a negative impact on ΔH). Therefore, the use of flexible spacers appears to be more promising, as they can compensate a certain degree of structural uncertainty. In this case, the intrinsic conformational entropy of the flexible spacer ΔS_{conf} has to be included into the model. As bivalent binding of the ligands will largely restrain spacer flexibility, it has to be added to the overall entropic cost. Once ΔS_{conf} is equal to or higher than the sum of ΔS_{trans} and ΔS_{rot} combined, the entropic enhancement will be marginal or vanish. As a consequence, this kind of bivalent ligand has either the same affinity as the monovalent ligand, or a weaker one.

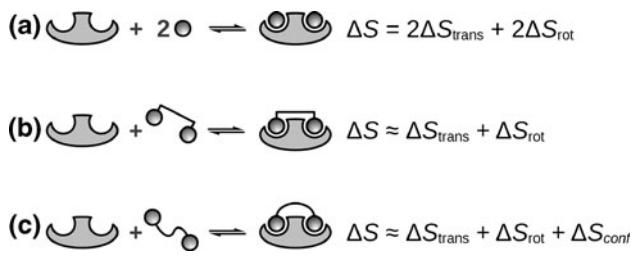

Fig. 1 Simplified model of bivalent binding, where we assume that ΔS_{trans} and ΔS_{rot} remain invariant from case to case. **a** Monovalent ligands **b** Bivalent ligand bridged by a rigid spacer **c** Bivalent ligand bridged by a flexible spacer

In 1994, Bergmann et al. first investigated the effects of a series of bivalent hexestrol (a nonsteroidal ER agonist) linked with varying lengths of oligomethylene and oligo(ethylene glycol) (OEG) [3]. During the last two decades, several bivalent ER ligands, composed of two individual ligands linked by flexible tethers, have been designed and synthesized [4, 10, 22]. In 2010, Wendlandt *et al*. showed the biological activity of synthetic bivalent estrogen dimers linked by aliphatic spacers to be higher than that of 17β-estradiol [33]. Unfortunately, whenever receptor binding affinity was measured, bivalent compounds mostly gave poor potencies, significantly below the level of their monovalent counterparts. When comparing different tether lengths, however, binding affinities were peaking at the distance of the optimal bivalent interaction. Based on the simple model of bivalent binding introduced above, it can be assumed that the drop in binding affinity can be attributed to the additional entropic cost intrinsic to flexible spacers, or a lack of structural fitness of the bivalent compounds that is related to the spacer, or a combination of both.

A better understanding of these factors is a prerequisite for the development of potent bivalent ligands that can actually fulfill the promise of enhanced binding affinity. In this article, we assess the structural and entropic properties of different flexible and semi-flexible spacer types based on OEG by means of conformational sampling and conformational entropy calculations. Furthermore, we investigate how ligand and spacer may interact in aqueous solution. In the end, we want to give certain guidelines for the design of bivalent ligands.

Spacer design

Looking for design paradigms

The most important factor for spacer design is the effective distance that has to be bridged, i. e. the distance between the target binding sites. In case of ERα, crystal structures reveal the binding site centers to be approximately 31 Å apart, while the straight-line distance between the binding site openings of the SERM binding conformation is approximately 34.5 Å (measured in RCSB-PDB file 2R6W [8]). The ER dimer is a relatively rigid structure, so that we can assume the binding site distance to remain constant. However, there exist multiple binding site proteins with flexible interdomains where this assumption can not be made.

Another determining factor for spacer design is spacer flexibility. The spacer has to be flexible enough to permit the attached ligands to enter the target binding site. The spacer should not create additional energy barriers that

impede the binding of the ligands. In this respect, flexible spacers such as OEG appear to be most adequate. More flexibility of the spacer comes at the cost of increased conformational entropy ΔS_{conf}, which in turn penalizes binding affinity.

A third factor to be considered is related to interactions of the spacer with itself and the attached ligands, which again is determined by spacer flexibility (as such interactions can only occur if spacer flexibility allows for it). Ligand-ligand interactions may occur if the spacer folds over so that the attached ligands can come into interaction range. Ligand-spacer interactions may occur if, for example, both ligand and spacer possess hydrophobic motifs, and, finally, the spacer may form superstructures such as helices by self-interaction. All of these effects are likely to penalize binding affinity.

There is an abundance of other questions related to the design of molecular spacers, such as uptake, processing in biological systems, and, of course, chemical synthesis. These, however, are beyond the focus of this article.

OEG spacers and novel semi-flexible spacer designs

So far, the most commonly used spacer for bivalent inhibition of ER has been OEG or PEG (poly(ethylene glycol)). It is water-soluble, has a low toxicity and is commercially available in different chain lengths. However, as was briefly discussed in the introduction, the performance of OEG-linked bivalent ER ligands still leaves room for improvement. It was shown that OEG has a flexible structure that is prone to form coiled and helix-like conformations in aqueous solution [21]. This property may be disadvantageous for the applicability of OEG/PEG as a molecular spacer. LaFrate et al. proposed the use of less polar compounds (poly(propylene) and poly(butylene glycol) ethers) to address the challenge of coil and helix formation. This, too, did not immediately lead to improved binding affinities. In this article, we compare the basic EG11 spacer to five OEG-based spacer designs, which, in fully extended conformation, are bridging approximately the same distance as EG11 (compare Table 2). The new designs introduce different structural motifs to the OEG backbone, meant to break helical folding patterns and provide rigidity for the extended, distance-spanning conformations one is typically looking for. For rigid elements, we use 2-butyne (spacers 3, 5 and 6), phenyl (spacer 5) and biphenyl (spacers 4 and 6), as summarized in Fig. 2. Regarding spacer design 2, no additional rigidity is added to the structure, but the central EG subunit is replaced by a single carbon-carbon bond, again meant to suppress helix formation. A conformational analysis of all compounds is performed to assess the effect of the proposed structural elements. Furthermore, we will apply a method for entropy estimation [32] to look into the impact of rigid elements on the entropy characteristics. By retaining OEG as structural element in all of the proposed spacer designs, we want to maintain sufficient solubility in water. Attaching ligands to a flexible or semi-flexible spacer is likely to have an impact on its conformational profile. Unwanted interactions between ligand and ligand as well as ligand and spacer may be related to the low binding affinities that so far have been reported for bivalent ER ligands. To look into this, we modeled each of the proposed spacer designs once without ligand attached, capped only with bromine (see Fig. 2), and once coupled via amide to DES (see Fig. 3, with bivalent DES-coupled EG11 serving as an example). Note that in the context of this article, DES serves merely as a prominent representative for any ER binding ligand.

Table 1 Overview of spacer designs 1 to 6 and their maximum spanned distance in fully extended conformation

#	Spacer structure	Length (Å)
1	EG11	43.72
2	EG5-C_2-EG5	42.59
3	EG5-(2-butyne)-EG5	42.60
4	EG5-C-biphenyl-C-EG5	48.59
5	EG4-(2-butyne)-O-phenyl-O-(2-butyne)-EG4	44.84
6	EG3-(2-butyne)-O-biphenyl-O-(2-butyne)-EG3	45.31

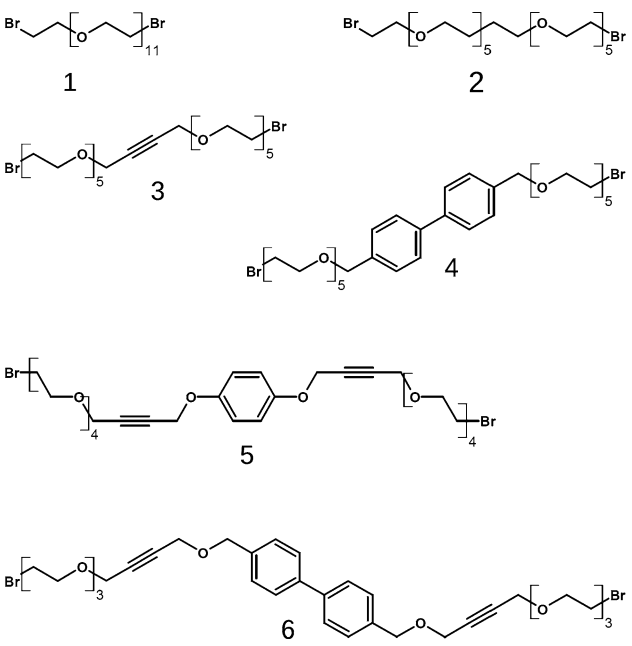

Fig. 2 Besides bromine-capped EG11 (compound 1), our studies include the compounds 2 to 6, depicted above. In a fully extended conformation, all compounds span distances of approximately 42 to 48 Å

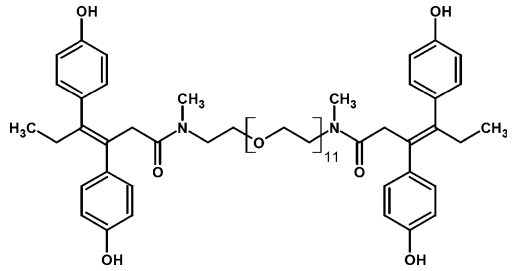

Fig. 3 DES coupled via amide to EG11, forming a bivalent ligand for ER. For comparison, each spacer design shown in Fig. 2 was modeled with and without ligands attached (i. e. amide-coupled to DES or bromine-capped)

Methods

Modeling and simulation

Spacer and bivalent ligand structures were modeled using the visualization software Amira [29]. The structures were solvated with roughly 20,000 water molecules each, in equally sized rhombic dodecahedron boxes of 9.6 nm side length. The energy of the systems was minimized with the steepest descent algorithm, and 200 ps simulations were performed during which the positions of all heavy spacer and ligand atoms were restrained. These systems were subsequently used as starting conformations for MD simulations of 100 ns length per structure. We used the Amber-99SB forcefield [15] with the TIP4P-Ew water model [14]. All structures were parameterized using the software Antechamber from AmberTools 1.2 [7, 30, 31], with charges calculated by the AM1-BCC method [16, 17]. To maintain a constant temperature of 300 K and a pressure of 1 bar, velocity rescaling [6] and Berendsen weak coupling [2] were applied. A twin range cut-off of 1.0/1.4 nm for van der Waals interactions was applied and the smooth particle mesh Ewald algorithm [9] was used for Coulomb interactions, with a switching distance of 1.0 nm. Bond lengths were contrained using the LINCS algorithm [12], allowing for an integration step of 2 fs. All simulations were performed using the GROMACS 4 software [13] and the according port of the Amber forcefields, ffamber [28].

Conformational entropy estimation

In order to determine differences in the conformational entropy ΔS_{conf} of the spacer designs in question, we employ the approach of Weber and Andrae [32], who derived the following formula to approximate the entropy difference ΔS between two molecular systems 1 and 2:

$$\Delta S \approx k_B \ln\left(\frac{M_1 \sum_{j=1}^{M_2}[U_{vol_2}(q_j^{(2)})]^{-1}}{M_2 \sum_{j=1}^{M_1}[U_{vol_1}(q_j^{(1)})]^{-1}}\right) \quad (1)$$

In the above formula, k_B is Boltzmann's constant, and $q_j^{(i)} \in \Omega_i$, with Ω_i being the conformational space of system i ($i = 1,2$), is a set of M_i representative conformational states. A conformational state is considered representative, if the potential energy value of this state is approximately equal to the mean potential energy value of the according set of Boltzmann distributed states $q^{(i)}$, i. e.

$$V_i(q_j^{(i)}) \approx \langle V_i(q^{(i)})\rangle \forall j. \quad (2)$$

In Eq. 1, the expression $U_{vol_i}(q_j^{(i)})$ counts the number of conformational states which is found inside a certain environment vol_i of a representative state $q_j^{(i)}$, or, in other words, the local density of sampling points. This approach is based on the observation that entropy manifests in the scattering of sampling data. To apply the method, we require a sufficient, Boltzmann distributed sampling of conformation space, which in our case is obtained by thermostated MD simulation (compare section 1). In [32], the environment vol_i for density evaluation is defined in terms of an RMSD value given in Å, without definite guidelines on how to choose the size of vol_i. We introduce a slight change to this approach by defining a set of internal coordinates consisting of torsion angles and distances, and then calculating conformational distances with a metric in torsion angle and distance space. Based on the approach of Klimm et al. [20], for computing Eq. 1, we use the term

$$\left(U_{vol_i}(q_j^{(i)})\right)^{-1} \approx \frac{n^{(i)}}{n_{near}^{(i)} + 1} \quad (3)$$

where $n^{(i)}{}_{near}$ is the number of sampling points within distance vol_i of representative $q_j^{(i)}$, and $n^{(i)}$ is the total number of sampling points. Furthermore, we choose the size of vol_i to be equal to the variance of the defined internal coordinates. The variance is precomputed in a first iteration over the sampling data.

Note that in Eq. 1, vol_i has to be based on an equal number of coordinates, i. e. in order to be able to quantify entropy differences between structurally inequal systems, the estimate has to be based on equal or at least comparable substructures of the systems in question. Hence, for each of the spacer species, we select an equal number of backbone torsion angles apt to define the conformational state, as well as the spacer end-to-end distance (bromine-bromine for bromine-capped spacers, and nitrogen-nitrogen for ligand-coupled spacers) to define our set of internal coordinates. Triple bond torsion angles were accounted for with an entropy contribution of zero, as well as phenyl groups. Despite the structural similarity of the compounds under observation, we ended up with slightly different numbers of rotatable torsion angles per structure (ranging from 33 to 35). To improve the comparability of results, we padded up

the number of torsion angles by counting either one or two standard EG backbone torsion angles twice, where necessary, therewith artificially prolonging the EG portion of the spacer in a relatively minor way.

Conformational analysis

Conformation density plots were computed with the approach of Schmidt-Ehrenberg et al. [27] which is available as part of the visualization software Amira [29]. Rather than visualizing conformations in terms of a single representative, probability densities over all molecular geometries in the sampling data are accumulated and visualized by volume rendering. This requires the application of a suitable alignment of the geometries in advance, preferably along a rigid part of the molecule. Visualizing molecular conformations in terms of density plots helps to reveal molecular flexibility and metastable conformations.

Results

End-to-end distances

As Table 2 shows, mean end-to-end distances over 100 ns simulation time in water are less than half of what had been measured for the extended conformations. This indicates that folded spacer conformations are highly favored over linear conformations. The minimum observed troughout the trajectories is virtually equal for all spacer designs, which implies that all structures are flexible enough to fold over, i. e. the minimum end-to-end distance is limited only by the terminal bromines' Van der Waals raadi. The highest mean (denoted as μ) end-to-end distance is observed for spacer design 6, with 17.69 Å, which also has the highest standard deviation (denoted as σ), followed by EG11 (spacer design 1), with a mean of 14.99 Å. Maximum end-to-end distances reach more than 30 Å for all spacer designs, theoretically sufficient for bridging the two binding sites of ER. However, the occurence of extended conformations is very low (compare Fig. 4). The exception

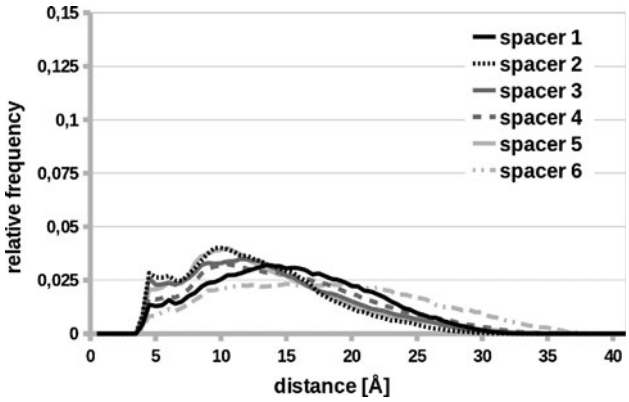

Fig. 4 Bromice-capped spacers: Histogram of bromine–bromine distances measured over 100 ns

is spacer design 6, where we also see the widest distribution of distances in general. End-to-end distances decrease further as soon as DES ligands are attached to the spacer (compare Table 3). Mean nitrogen-nitrogen distances are below 10 Å for all compounds, with spacer design 6 again performing best with 9.84 Å mean distance. We also find a general decrease of the standard deviation. Minimum and maximum distances remain relatively similar. Figure 5 shows that end-to-end distance distributions for ligand-coupled spacers become significantly narrower. The distinct peaks suggest that each compound adopts a relatively limited number of stable conformations. This especially seems to hold for spacer designs 1 to 4. The effects of ligand attachment on end-to-end distances mean and standard deviation for all compounds are summed up in Fig. 6. The largest drop of both mean and standard deviation on ligand attachment occurs for spacer design 6, followed by spacer design 4.

For comparison, we modeled the structure of a bivalent steroidal ligand published by LaFrate et al. [22], where an EG5 spacer connects two E_2s modified at the 17α position. Our data (not shown) suggests that this bivalent ligand also suffers from a drop in end-to-end distances (measured at the C17 positions) to a mean value distinctly below 10 Å. Hence, the effect does not seem to be limited to DES or similar SERMs only.

Table 2 Bromine-capped spacers: Bromine-bromine distance data measured over 100 ns, with mean μ and standard deviation σ

#	Min (Å)	Max (Å)	μ (Å)	σ (Å)
1	3.45	34.06	14.99	5.84
2	3.51	32.37	12.25	5.19
3	3.48	36.44	13.14	5.78
4	3.48	37.54	14.50	6.30
5	3.40	38.89	13.05	5.88
6	3.45	39.01	17.69	7.36

Table 3 DES-coupled spacers: Nitrogen-nitrogen distance data measured over 100 ns

#	Min (Å)	Max (Å)	μ (Å)	σ (Å)
1	3.61	31.19	9.53	3.75
2	4.06	29.81	9.72	2.27
3	3.11	31.52	8.11	2.86
4	3.71	33.03	8.55	3.34
5	3.48	40.84	9.33	3.82
6	3.36	35.07	9.84	3.44

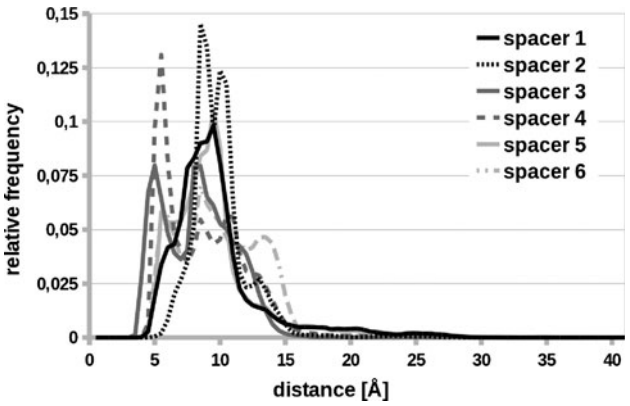

Fig. 5 Ligand-coupled spacers: Histogram of nitrogen-nitrogen distances measured over 100 ns

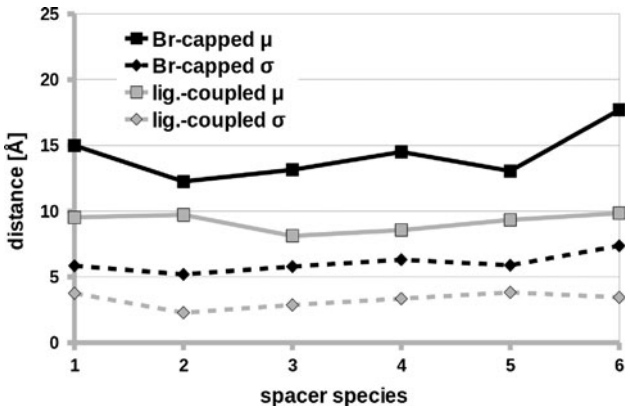

Fig. 6 Impact of ligand attachment on spacer end-to-end distance mean μ (*full line*) and standard deviation σ (*dotted line*). *Black*: bromine-capped compounds. *Light gray*: ligand-coupled compounds

Conformational entropy estimation

Conformational entropy follows an upward trend for spacer designs 1 to 6, where lowest conformational entropy is measured for spacer designs 1 and 2 (EG11 and its closest derivative), followed by spacer designs 3 and 4 (both containing either one 2-butyne or one biphenyl element). Spacer designs 5 and 6, which both contain combinations of multiple 2-butyne and phenyl elements, are ranking with the highest conformational entropy (compare Fig. 7). For all ligand-coupled compounds we find a lower conformational entropy than for their bromine-capped counterparts. This decrease is expected, as the results shown in Section 1 suggest that ligand-attachment constraints the conformations of the spacer. The extent of the entropy drop is most significant for spacer designs 4 and 6, which both contain biphenyl residues. The formation of stable hydrophobic interactions between biphenyl and DES ligands may explain this effect. By contrast, the smallest drop in conformational entropy is observed for spacer designs 1 and 2.

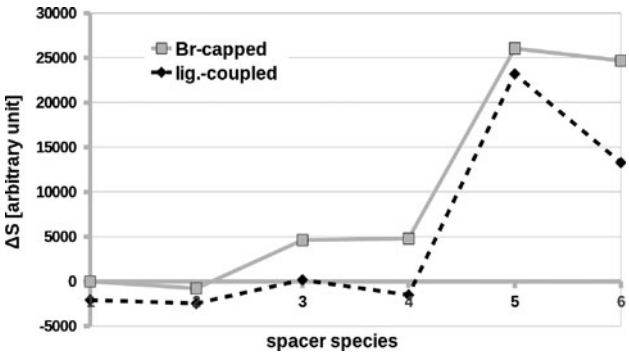

Fig. 7 Conformational entropy comparison, using bromine-capped EG11 (spacer design 1) as reference compound. *Full line*: bromine-capped spacers. *Dotted line*: ligand-coupled spacers

Here, either spacer structure may prohibit ligand-spacer and ligand-ligand interactions (which, however, would contradict end-to-end distance data), or the spacer intrinsically may have a folding pattern with low conformational entropy that is not dramatically altered as soon as ligands are attached. The latter seems to be the case for spacer designs 1 and 2, which in aqueous solution are prone to form low entropy helix-like structures.

The distinct rise of conformational entropy from spacer design 1 to 6 appears to be counterintuitive, as we introduced an increasing number of rigid, seemingly low entropy elements to the structures. In order to explain the ranking shown in Fig. 7, we looked into which structural elements contribute most to the spacers' conformational entropy balance (compare Fig. 8). The results of the entropy comparison are shown in Fig. 9. Highest entropy contribution is found for the terminal torsion angle of the spacer (CAP), where either bromine or the ligand is attached. One EG subunit consisting of three bonds has a relatively low entropy contribution, and shows a regular pattern of two low entropy torsions (EG1 and EG2) and one high entropy torsion (EG3). The second-highest entropy contribution can be found for torsions neighboring triple bonds (TRI), as they allow for unhindered rotation, resulting in an uniform distribution of the torsion angle. We also find high entropy contribution for torsions neighboring phenyl rings (PHE) and torsions connecting two phenyl rings (DPH). Therefore, although phenyl rings and triple bonds intrinsically are rigid, low entropy structures, they introduce high entropy to the system by enabling free rotation of the attached groups. Figure 9 suggests a relatively mild effect of ligand-attachment on individual torsion angle types, as all torsion types except EG2 remain more or less invariant. The significant drop in entropy for EG2 indicates that in spacer design 6 (which was used for the torsion angle comparison in Fig. 9) the biggest entropic penalty caused by ligand-spacer and ligand-ligand interactions has to be borne by the short EG3

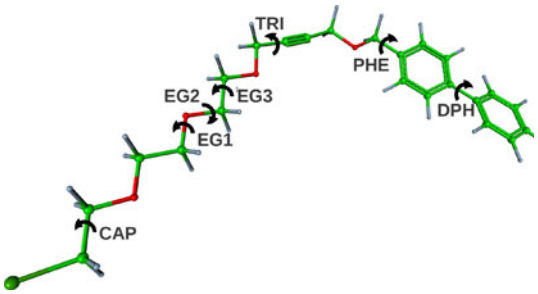

Fig. 8 Torsion angles with different entropy contribution: torsions at spacer caps or ends (CAP), torsions of EG units (EG1, EG2, EG3), torsions neighboring triple bonds (TRI), torsions neighboring phenyl rings (PHE), and torsions connecting two phenyl rings (DPH)

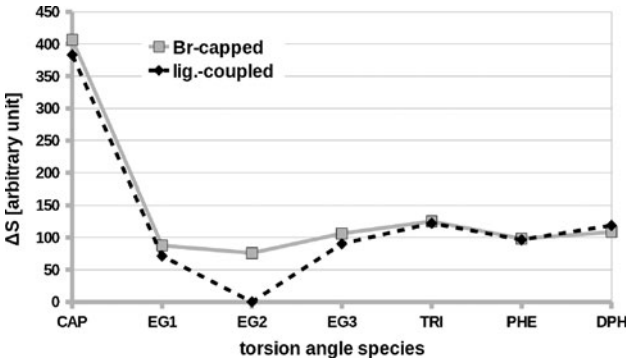

Fig. 9 Entropy contribution of different types types of torsion angles, measured on the example of spacer design 6. *Full line*: bromine-capped. *Dotted line*: ligand-coupled

chains, which otherwise would move freely. These results help to explain the conformational entropy ranking shown in Fig. 7: When an EG subunit is replaced by a triple bond (e. g. spacer design 3), two high entropy TRI torsions are introduced to the structure. This results in an overall higher conformational entropy, especially when the TRI motif interrupts a longer EG chain that otherwise would be prone to fold into a low entropy structure such as a helical loop. The same is true for structures containing phenyl (two PHE torsions) and biphenyl (two PHE torsions and one DPH torsion).

Conformational analysis

As the end-to-end distance results presented in Section 1 indicate, we can observe a folding of spacer structures in water. Predominant conformations for bromine-capped EG11 are either loop or U-shaped. Helical conformations are present in the mix, but we did not observe the formation of rigid helices that persist for more than a few picoseconds. The overall flexibility of EG seems to be high. For short EG chains, folding into complex coils or loops is not possible, which adds to the high flexibility. Rigid elements

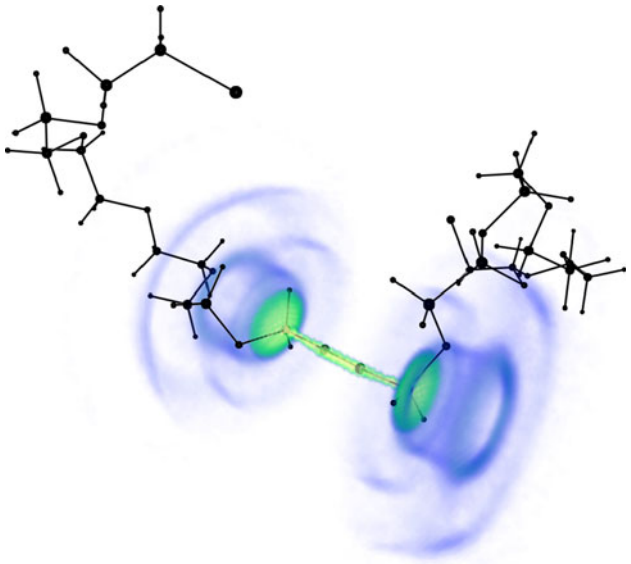

Fig. 10 Conformation density of bromine-capped spacer 3. Colouring indicates the presence of atoms with at least 10% probability. While the central 2-butyne fragment remains linear, the attached EG chains rotate heavily so that no distinct positions are visible

such as 2-butyne (compare Fig. 10) and biphenyl (data now shown) retain their linear conformation, but introduce a great amount of rotational entropy to the remaining part of the molecule. It can be argued that this free rotation might be favorable as it prevents trapping in a certain conformation. However, it leads to an increase of the entropy penalty at ligand binding. Depending on the spacer design, ligand-attachment can have more or less pronounced effects. For spacer design 3, we had calculated a relatively large drop in conformational entropy after coupling the spacer with DES ligands. This is supported by the conformation density plot shown in Fig. 11. While for the

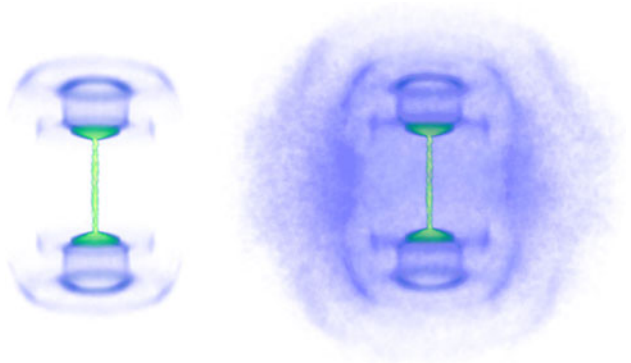

Fig. 11 Conformation density plot of spacer design 3. Colouring indicates the presence of atoms with at least 15% probability. *Left*: Without ligands attached, the EG chains can move freely. *Right*: With ligands attached, the structure becomes more compact and chain flexibility is restricted. The DES ligands align parallely to the 2-butyne part of the spacer, forming a barrel-shaped structure

bromine-capped spacer, EG chains can rotate freely, attaching DES ligands leads to a barrel-shaped structure, where DES aligns parallely to the 2-butyne part of the spacer. The molecule thus becomes more compact and less flexible. By contrast, for spacer design 5 we only found a relatively minor drop of conformational entropy after ligand-attachment. The according conformation density plot (compare Fig. 12) supports this finding, as with DES attached, the densities appear to be only slightly more defined than for the bromine-capped spacer. High rotation of the EG chains and the presence of only one aromatic ring in the structure of spacer design 5 may prevent the formation of more pronounced hydrophobic stacking interactions as in the case of biphenyl-containing spacer designs 4 and 6. For the spacer designs containing biphenyl, we found a variety of stacked conformations that maximize hydrophobic interactions with the DES ligands (see Fig. 13). This gives a justification for the low end-to-end distances that we observed (compare Section 1). The formation of stacked conformations not only neutralizes the distance spanned by the linear elements, but may also have adverse effects on water solubility. Although not taken into account within the course of these studies, it is possible that multiple structures can be involved in such interactions to form larger aggregates.

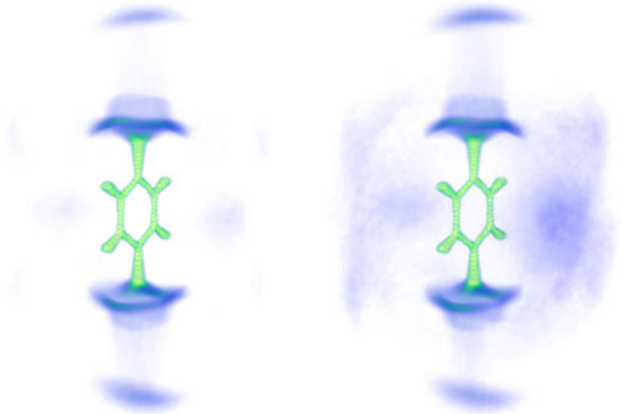

Fig. 12 Conformation density plot of spacer design 5. Colouring indicates the presence of atoms with at least 15% probability. We obtain a similar density plot for bromine-capped (*left*) and ligand-coupled spacers (*right*), i. e. the impact of ligand-attachment is relatively small. The slight shadows appearing parallel to the phenyl ring indicate the presence of the ligands or parts of the spacer interacting with the phenyl ring. The fact that the density cloud in this area is not very defined suggests that these interactions are comparatively weak, i. e. conformational flexibility remains. This is in agreement with the conformational entropy estimation of spacer design 5, where only a minor entropy drop after ligand-attachment was found

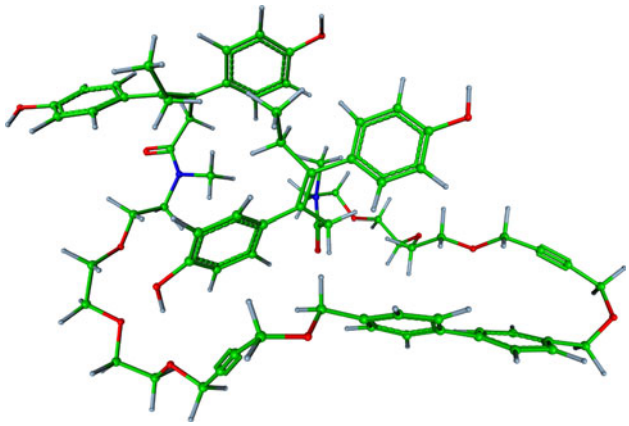

Fig. 13 Ligand-coupled spacer 6 in water: Hydrophobic interactions promote stacked, sandwich-like conformations

Discussion

The design of potent bivalent ligands for ER remains a challenging task. The ligand binding sites are buried deeply within the receptor, and between the binding sites a distance of more than 30 Å has to be bridged. The molecular spacer used to connect the ligands has to provide the right interplay between flexibility and rigidity.

Our studies suggest that an optimal spacer should be as rigid as possible while still providing the flexibility that is needed. Furthermore, in order to provide reliable design guidelines for chemists, the spacer should have a defined conformation and bridging distance when in solvent, and the spacer parameters should be invariant to the attachment of ligands. The spacers under investigation in this article reveal certain weaknesses. Due to their high flexibility, the effective bridging distance in water is diminished even after introducing rigid segments. As OEG/PEG shows very variable folding patterns, a mere prolonging of the chain is only of limited use. The prediction of an optimal chain length is not possible without elaborate case-specific analysis. Furthermore, the attachment of ligands leads to distinct changes of the spacers' parameters, which complicates the rational design of bivalent ligands.

Conformation density plots show that the use of phenyl and 2-butyne as linear, rigid elements leads to more defined spacer structures and linear conformations. The positive effects are neutralized, however, by the flexibility of the attached OEG chains. Even short chains of three EG units allow for enough flexility to permit interactions between the ligand and hydrophobic parts of the spacer.

As a consequence, we feel the need for hydrophilic and yet rigid compounds that can be assembled in a modular fashion to provide spacer structures with defined conformation and bridging distance. In order to prohibit ligand-

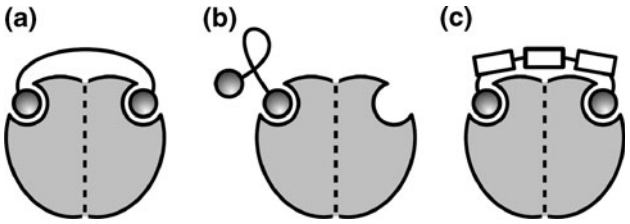

Fig. 14 Different scenarios of bivalent binding where the spacer can have an impact: **a** Bivalent binding with flexible spacer, spacer adapts linear conformation **b** Inhibition of bivalent binding due to folding and aggregation of the flexible spacer **c** Bivalent binding with modular rigid spacer and short flexible linkers. *Note* that the length of the flexible linker connecting ligand and spacer has to suffice to allow ligand access to the binding site without causing steric hindrance between spacer and the ER surface. The required linker length is dependent on the structure of the ligand. Our exemplary ligand DES is buried deeply in the ER structure and thus requires a linker of several Å length, whereas larger SERMs such as raloxifene protrude from the binding pocket so that only a very short linker is required

spacer interactions that might hinder the free presentation of the ligands required for binding to the target, the flexible linker used to connect spacer and ligand ought to be rather short (compare Fig. 14).

The main promise of bivalent (and multivalent ligands in general) is the entropic advantage regarding ΔS_{trans} and ΔS_{rot} over their monovalent counterparts. This advantage is reduced by the intrinsic entropy contribution of the spacer, ΔS_{conf}. We performed conformational entropy calculations in order to look into ΔS_{conf} of different spacer types and elements. For OEG chains, we found a regular pattern of triples consisting of two low entropy torsions and one high entropy torsion. For phenyl and biphenyl, we found hardly any entropy contribution of torsions involved in the aromatic systems. However, bonds neighboring aromatic rings allow for unhindered rotation. The same holds for bonds neighboring triple bonds. Although 2-butyne and phenyl/biphenyl parts help to construct rigid, linear structures that maintain defined distances for ligand presentation, their high contribution to ΔS_{conf} appears to be a drawback. In general, we computed higher ΔS_{conf} values for spacers containing 2-butyne and phenyl elements.

As depicted in Fig. 14, our results suggest that the probability to find the system in state a) is low, as the occurence of extended spacer conformations is low, whereas folded spacer conformations, as shown in b), occur with high probability. The use of rigid, modular spacer scaffolds with defined ligand presentation distance and short flexible linkers as shown in c) may offer the best compromise of flexibility and rigidity.

The entropic advantage that leads to a positive cooperative effect can only be exploited if the spacer does not interfere with ΔH, i. e. the ligands should be presented in a way that allows unhindered access to the target binding sites. Therefore, maintaining a defined ligand-ligand distance (corresponding to the approximate binding site displacement) and avoiding ligand-ligand interactions that interfere with ligand presentation (such as hydrophobic stacking) is more fundamental than entropic optimization of the spacer.

An issue not addressed in this study, but currently under observation, is the interplay of protein and spacer structure. One might imagine a scenario where contact between spacer and protein (e. g. following a monovalent binding event) induces spacer-protein interactions that promote unfolding of the flexible spacer, thus leading to linear spacer conformations that encourage bivalent binding. Furthermore, these interactions might even improve the binding energy term so that $\Delta H_{bi} \approx 2 \times \Delta H_{mono} + \Delta H_{spacer}$. Regarding the use of PEG spacers this scenario can be challenged, as PEG, when attached to surfaces, is known to have strong protein-repellent properties [11]. This, however, should be the subject of further investigations.

The results presented in this article may be helpful in order to avoid certain traps connected with the design of bivalent ligands for ER, or similar bivalent targets. Our findings may serve as starting points for research to provide chemists with new and improved molecular spacer structures.

Acknowledgments Support by the Deutsche Forschungsgemeinschaft (SFB 765) is gratefully acknowledged.

References

1. Avendano C, Menendez JC (2008) Medicinal chemistry of anticancer drugs. Elsevier B.V., Amsterdam
2. Berendsen HJC, Postma JPM, DiNola A, Haak JR (1984) Molecular dynamics with coupling to an external bath. J Chem Phys 81:3684–3690
3. Bergmann KE, Woogef CH, Carlson KE, Katzenellenbogen BS, Katzenellenbogen JA (1994) Bivalent ligands as probes of estrogen receptor action. J Steroid Biochem Mol Biol 49:139–152
4. Berube G, Rabouin D, Perron V, N'Zemba B, Gaudreault RC, Parent S, Asselin E (2006) Synthesis of unique 17β-estradiol homo-dimers, estrogen receptors binding affinity evaluation and cytocidal activity on breast, intestinal and skin cancer cell lines. Steroids 71:911–921
5. Brzozowski AM, Pike ACW, Dauter Z, Hubbard RE, Bonn T, Engstroem O, Oehman L, Greene GL, Gustafsson J, Carlquis M (1997) Molecular basis of agonism and antagonism in the oestrogen receptor. Nature 389:753–758
6. Bussi G, Donadio D, Parrinello M (2007) Canonical sampling through velocity rescaling. J Chem Phys 126:14–101
7. Case D, III, TEC, Darden T, Gohlke H, Luo R, Jr., KMM, Onufriev A, Simmerling C, Wang B, Woods R (2005) The Amber biomolecular simulation programs. J Comput Chem 26:1668–1688
8. Dai SY, Chalmers MJ, Bruning J, Bramlett KS, Osborne HE, Montrose-Rafizadeh C, Barr RJ, Wang Y, Wang M, Burris TP, Dodge JA, Griffin PR (2008) Prediction of the tissue-specificity

of selective estrogen receptor modulators by using a single biochemical method. Proc Natl Acad Sci 105(20):7171–7176
9. Essmann U, Perera L, Berkowitz ML, Darden T, Lee H, Pedersen LG (1995) A smooth particle mesh Ewald method. J Chem Phys 103:8577–8592
10. Groleau S, Nault J, Lepage M, Couturea M, Dallaire N, Berube G, C-Gaudreault R (1999) Synthesis and preliminary in vitro cytotoxic activity of new triphenylethylene dimers. Bioorg Chem 27(5):383–394
11. Lee HJ, Lee HB, Andrade JD (1995) Blood compatibility of polyethylene oxide surfaces. Prog Polym Sci 20:1043–1079
12. Hess B, Bekker H, Berendsen HJC, Fraaije JGEM (1997) LINCS: a linear constraint solver for molecular simulations. J Comput Chem 18:1463–1472
13. Hess B, Kutzner C, van der Spoel D, Lindahl E (2008) GROMACS 4: algorithms for highly efficient, load-balanced, and scalable molecular simulation. J Chem Theory Comput 4(3): 435–447
14. Horn HW, Swope WC, Pitera JW, Madura JD, Dick TJ, Hura GL, Head-Gordon T (2004) Development of an improved four-site water model for biomolecular simulations: TIP4P-Ew. J Chem Phys 120:9665–9678
15. Hornak V, Abel R, Okur A, Strockbine B, Roitberg A, Simmerling C (2006) Comparison of multiple Amber force fields and development of improved protein backbone parameters. Proteins 65:712–725
16. Jakalian A, Bush BL, Jack DB, Bayly CI (2000) Fast, efficient generation of high-quality atomic charges. AM1-BCC model: I. Method. J Comput Chem 21:132–146
17. Jakalian A, Jack DB, Bayly CI (2002) Fast, efficient generation of high-quality atomic charges AM1-BCC model: II Parameterization and validation. J Comput Chem 23:1623–1641
18. Jordan VC (2003) Antiestrogens and selective estrogen receptor modulators as multifunctional medicines. 1. Receptor interactions. J Med Chem 46:883–903
19. Jordan VC (2003) Antiestrogens and selective estrogen receptor modulators as multifunctional medicines. 2. Clinical considerations and new agents. J Med Chem 46:1081–1111
20. Klimm M, Bujotzek A, Weber M (2010) Direct reweighting strategies in conformation dynamics. MATCH Commun Math Comput Chem 65(2) (in press)
21. Kreuzer HJ, Wang RLC, Grunze M (1999) Effect of stretching on the molecular conformation of oligo (ethylene oxide): a theoretical study. New J Phys 1:21.1–21.16
22. LaFrate AL, Carlson KE, Katzenellenbogen JA (2009) Steroidal bivalent ligands for the estrogen receptor: design, synthesis, characterization and binding affinities. Bioorg Med Chem 17:3528–3535
23. Mammen M, Choi S, Whitesides GM (1998) Polyvalent interactions in biological systems: Implications for design and use of multivalent ligands and inhibitors. Angew Chem Int Ed 37: 2754–2794
24. Ottow E, Weinmann H (2008) Nuclear receptors as drug targets. WILEY-VCH Verlag GmbH & Co. KGaA, Weinheim
25. Rao J, Lahiri J, Weis RM, Whitesides GM (2000) Design, synthesis, and characterization of a high-affinity trivalent system derived from vancomycin and L-Lys-D-Ala-D-Ala. J Am Chem Soc 122:2698–2710
26. Salomonsson M, Häggblad J, O'Malley BW, Sitbon GM (1994) The human estrogen receptor hormone binding domain dimerizes independently of ligand activation. J Steroid Biochem Mol Biol 48:447–452
27. Schmidt-Ehrenberg J, Baum D, Hege HC (2002) Visualizing dynamic molecular conformations. In: Proceedings of IEEE visualization 2002. IEEE Computer Society Press, pp 235–242
28. Sorin EJ, Pande VS (2005) Exploring the helix-coil transition via all-atom equilibrium ensemble simulations. Biophys J 88(4): 2472–2493
29. Stalling D, Westerhoff M, Hege HC (2005) Amira: a highly interactive system for visual data analysis. In: Hansen CD, Johnson CR (eds) The visualization handbook, chap. 38. Elsevier, UK, pp 749–767
30. Wang J, Wang W, Kollman PA, Case DA (2006) Automatic atom type and bond type perception in molecular mechanical calculations. J Mol Graphics Model 25:247–260
31. Wang J, Wolf RM, Caldwell J, Kollman PA, Case DA (2004) Development and testing of a general Amber force field. J Comput Chem 25:1157–1174
32. Weber M, Andrae K (2010) A simple method for the estimation of entropy differences. MATCH Commun Math Comput Chem 63(2):319–332
33. Wendlandt AE, Yelton SM, Lou D, Watt DS, Noonan DJ (2010) Synthesis and functional analysis of novel bivalent estrogens. Steroids 75:825–833